Distributed Cooperative Voltage Control of Networked Islanded Microgrid via Proportional-Integral Observer

Shen Yan, Zhou Gu, *Senior Member, IEEE*, Ju H. Park, *Senior Member, IEEE*, Xiangpeng Xie, *Senior Member, IEEE*, and Wei Sun, *Senior Member, IEEE*

***Abstract*—This article is concerned with the proportional-integral observer-based distributed cooperative voltage control issue of the networked islanded microgrid subject to probabilistic communication delay. Due to the fact that the reference signal is usually received by partial distributed generators, the system model with a constant reference signal in some existing results is difficult for control synthesis. To solve this problem, a distributed control law based on the measured voltage is designed to estimate the reference signals for all distributed generators. Then, by treating the deviation between the estimated and measured voltages as the small signal, a novel small-signal model of the networked microgrid voltage control system is established. With the utilization of the probabilistic feature of communication delay, a distribution-dependent delay handling manner is taken into account. To improve the estimation accuracy of the system state, a proportional-integral observer is adopted based on the local measured voltage. With the aid of Lyapunov theory and linear matrix inequality technology, sufficient criteria are proposed for co-designing the controller and observer gains to guarantee that the reference voltage is tracked by all distributed generators. Lastly, some simulation results are carried out to manifest the merits of the developed strategy.**

***Index Terms*—Networked microgrid, distributed cooperative voltage control, proportional-integral observer, probabilistic communication delay, controller and observer co-design.**

Manuscript received 12 June 2023; revised 26 October 2023 and 21 February 2024; accepted 27 May 2024. Date of publication 31 May 2024; date of current version 23 October 2024. This work was supported in part by the National Natural Science Foundation of China under Grant 62103193, Grant 62273183, Grant 62373196, and Grant 52277087; and in part by the Natural Science Foundation of Jiangsu Province of China under Grant BK20200769, Grant BK20231288, and Grant BK20231286. The work of Ju H. Park was supported by the National Research Foundation of Korea (NRF) Grant funded by the Korea Government (Ministry of Science and Information and Communications Technology) under Grant 2019R1A5A8080290. Paper no. TSG-00856-2023. *(Corresponding authors: Zhou Gu; Ju H. Park; Xiangpeng Xie.)*

Shen Yan is with the College of Mechanical and Electronic Engineering, Nanjing Forestry University, Nanjing 210037, China (e-mail: yanshenzdh@gmail.com).

Zhou Gu is with the School of Electrical Engineering, Anhui Polytechnic University, Wuhu 241000, China (e-mail: gzh1808@163.com).

Ju H. Park is with the Department of Electrical Engineering, Yeungnam University, Gyeongsan 38541, South Korea (e-mail: jessie@ynu.ac.kr).

Xiangpeng Xie is with the School of Internet of Things, Nanjing University of Posts and Telecommunications, Nanjing 210023, China (e-mail: xiexiangpeng1953@163.com).

Wei Sun is with the School of Electrical and Automation Engineering, Hefei University of Technology, Hefei 230009, China (e-mail: wsun@hfut.edu.cn).

Color versions of one or more figures in this article are available at https://doi.org/10.1109/TSG.2024.3407770.

Digital Object Identifier 10.1109/TSG.2024.3407770

I. Introduction

THE MICROGRID represents a small scale power system that integrates distributed renewable energy resources and loads efficiently. There are two main operation patterns of microgrids: grid-connected pattern and islanded pattern. In the presence of unexpected disconnection between the microgrid and main power grid, the microgrid will turn into islanded operation. However, under the islanded mode, the voltage and frequency stabilities of the microgrid, which are maintained via the traditional droop control strategy, could be degraded even destroyed [1], [2]. In order to handle this problem, secondary control strategy has gained more and more attention in recent years. There are three typical types of secondary control strategy: centralized control [3], decentralized control [4] and distributed control [5], [6], [7], respectively. Due to the advantage of low communication and calculation burden between the distributed generators (DGs), distributed secondary cooperative control becomes more popular than the others [8], [9].

In [10], a distributed secondary cooperative control scheme is presented to regulate the frequency and voltage of an islanded microgrid. A distributed observer is introduced to estimate the reference voltage signal for all DGs in [11], where the voltage restoration is realized by applying model predictive control based on the estimated signal. With the introduction of communication networks in these results, network-induced communication delay is an unavoidable factor. This delay may not only degrade consensus performance but also lead to instability of multi-agent systems. [12] studies the consensus problem of heterogeneous linear multi-agent systems with time-varying communication delays using a dynamic periodic event-triggered approach. The event-triggered consensus issue of multiple Euler–Lagrange systems subject to unavailable velocity information and communication delays is addressed in [13]. The finite-time observer-based leader-following consensus issue is investigated in [14] studies for nonlinear multi-agent systems with time-varying input delays. Considering the typical application of multi-agent consensus issue, the voltage restoration of networked microgrid systems with communication delays has been explored in [15], [16], [17]. To be specific, [15] studies a distributed voltage control scheme for DC microgrids subject to constant communication delays. In [16], the multi-agent-system-based distributed control problem of DC microgrid with switching topology communication network and time-varying communication delay is investigated. Meanwhile, the global voltage regulation and proportional current sharing are achieved. In [17], a droop-based distributed cooperative voltage/frequency restoration strategy is proposed for microgrids with time-varying delays under a switching communication. It is worth noting that the above results only consider constant or time-varying communication delays. In practical networked microgrids, communication delays are usually complex and stochastic with some probabilistic features [4], [18], [29], [30]. Recently, some interesting outcomes about distributed voltage/frequency control for networked microgrids with stochastic time-varying delays are derived in [19], [20]. Specifically, a Markov process is used to describe the stochastic feature of communication delay, and a small-signal microgrid model for the voltage/frequency regulation system is proposed in [19]. By considering both random communication delay and rapid switching communication topology, some stability analysis conditions based on a secondary distributed control strategy for the microgrid are provided in [20]. However, the small-signal model established in the aforementioned results [19], [20] includes constant reference voltage and frequency signals. The control parameters are manually chosen and tuned by designers without theoretical analysis. Consequently, how to design the controller gains theoretically under a microgrid voltage control system with probabilistic communication delay and without constant reference signal is the first motivation of this study.

For microgrid control systems, it is usual to design a controller based on the measured voltage and frequency information. This is viewed as an output control scheme. Compared with the output control scheme, a state feedback controller is potential to yield superior control performance. As a result, various results have concentrated on observer design, which utilizes measured outputs to estimate the full state of networked control systems [21], [22], [23]. Two fundamental types of observers are prevalent: the Kalman filter-based observer and the Luenberger observer. In contrast to the Kalman filter with four computation equations and exact knowledge of random noises, the Luenberger observer usually requires only one dynamic equation and incurs less computation burden. For a DC microgrid with multiple interconnected DGs, a distributed Luenberger observer is applied to solve the fault detection issue in [24]. Considering a cyber-physical microgrid subject to false data injection, a resilient frequency regulation scheme is designed in [25], where a Luenberger observer is utilized to acquire the estimations of the unknown input and state simultaneously. In order to increase the observation accuracy of state variables, a proportional-integral observer (PIO) with an extra integral term is investigated in [26], [27], [28]. To our best knowledge, nevertheless, the PIO-based voltage control problem for networked microgrids with probabilistic communication delay has not been studied in existing literature, which is the second motivation of the present work.

This article studies the distributed PIO-based voltage control issue for networked microgrids with probabilistic communication delay. The main contributions are summarized as follows:

1) A novel small-gain signal model of the networked microgird voltage control system is established. Under this model, a distributed control law is designed to estimate the reference voltage signal for all DGs. By treating the deviation between the measured and estimated voltage signals as the small signal, the proposed new model removes the constant reference voltage signal in the existing small-signal model in [19], [20]. Then, it can be used for stability analysis and the co-design of controller gains and some required control performances.

2) The stability analysis conditions for networked microgrid voltage control system with probabilistic communication delay are derived by using the PIO. In some existing results about control problems of networked microgrids, the communication delay is considered as constant delay [15] or time-varying delay [16], [17]. However, it is usually stochastic with some distribution features. In order to make full of use the stochastic feature, the probability distribution of communication delay is utilized in the delay modeling. Therefore, compared to the existing results [15], [16], [17], our distribution-dependent delay (DDD) handling method is able to derive less conservative results. In addition, a PIO using the extra integral information rather than the conventional proportional observer (PO) is studied to improve the state estimation accuracy.

3) According to the above derived stability conditions, some co-design conditions for the controller and observer gains are deduced by a set of linear matrix inequalities (LMIs). In previous outcomes [19], [20], the controller gains are selected and tuned manually based on the designer experience, which can not be designed theoretically. The proposed theoretical controller design method surpasses the existing manual design approach in [19], [20].

The rest content of this paper is organized as follows. The system modeling and problem statement is presented in Section II. The stability analysis and controller design conditions for networked islanded microgrids are derived in Section III. Simulation results are shown in Section IV. Conclusions are summarized in Section V.

Notation: In the paper, $\mathbf{He}(P)$ stands for $P + P^{\top}$, where $P^{\top}$ denotes the transpose of matrix P. $\mathbf{Sy}(Y, X) \triangleq X^{\top}YX$. Kronecker product is represented by $\otimes$. $\left[x_i(t)\right]_N$ means $\left[x_1^{\top}(t) \cdots x_i^{\top}(t) \cdots x_N^{\top}(t)\right]^{\top}$. $\mathbb{E}\{\lambda(t)\}$ means the mathematical expectation of the random variable $\lambda(t)$.

II. System Modeling and Preliminaries

A. Graph Theory

Taking into account an islanded microgrid with N DGs, the communication network is modeled as a directed graph $\mathbf{G} = \{\mathbf{V}, \mathbf{E}\}$, in which $\mathbf{V} = \{1, 2, \ldots, N\}$ represents the set of nodes and $\mathbf{E} \in \mathbf{V} \times \mathbf{V}$ stands for the set of communication links between DGs. $\mathbf{A} = [a_{ij}] \in \mathbb{R}^{N\times N}$ is an adjacency matrix, where $a_{ij} = 1$ and $a_{ij} = 0$ for $i \neq j$ mean node i and node j are adjacent and not adjacent, respectively, and $a_{ii} = 0$ for any $i \in \mathbf{V}$. $N_i = \{j \in \mathbf{V} : (i, j) \in \mathbf{E}\}$ stands for the set of neighbors of the i-th DG. The degree matrix of $\mathbf{G}$ is represented by $\mathbf{W} = diag\{w_1, w_2, \ldots, w_N\}$, in which the in-degree of node i equals to $w_i = \sum_{j\in N_i} a_{ij}$. Then, the Laplacian matrix of $\mathbf{G}$

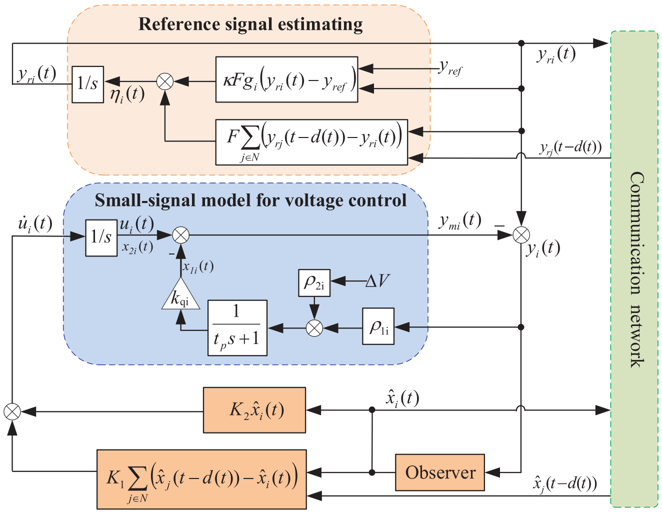

Fig. 1. The framework of voltage control for a networked islanded microgrid based on small-signal model.

is defined as $\mathbf{L} = \mathbf{W} - \mathbf{A}$. The pining gain matrix is $G = diag\{g_1, g_2, \ldots, g_N\}$.

B. Microgrid Voltage Control System Modeling

In terms of microgrid voltage control system established via the small-signal model in the existing literature [19], [20], the framework for networked microgrid voltage control, utilizing a new small-signal model that incorporates the estimated reference signal, is depicted in Fig. 1.

In a real islanded microgrid, it is common that only part of DGs can obtain the reference signal, but at least one DG can receive it [19], [20]. A small-signal system model with constant reference signal is established in existing results [19], [20] to deal with the voltage consensus problem. This microgrid model can not be utilized for the theoretic co-design of controller gains and some required control performances. In order to overcome this difficulty, the following distributed control law is designed to obtain the reference voltage signals for all DGs as

$$\begin{aligned}\dot{y}_{ri}(t) &= F\sum_{j\in N_i} a_{ij}\big[y_{rj}(t-d(t)) - y_{ri}(t)\big] \\ &\quad + \kappa F g_i\big(y_{ri}(t) - y_{ref}\big) \\ &= F\sum_{j\in N_i} a_{ij}\Big[\big(y_{rj}(t-d(t)) - y_{ref}\big) - \big(y_{ri}(t) - y_{ref}\big)\Big) \\ &\quad + \kappa g_i\big(y_{ri}(t) - y_{ref}\big)\Big],\end{aligned} \tag{1}$$

where $y_{ri}(t)$ represents the estimated reference signal for the ith DG, F and κ are control parameters to be chosen.

By setting $z_i(t) = y_{ri}(t) - y_{ref}$, $z_i(t-d(t)) = y_{ri}(t-d(t)) - y_{ref}$, it yields

$$\begin{aligned}\dot{z}_i(t) &= F\sum_{j\in N_i} a_{ij}\big[z_j(t-d(t)) - z_i(t) + \kappa g_i z_i(t)\big] \\ &= F\sum_{j\in N_i} a_{ij}\big[z_j(t-d(t)) - z_i(t-d(t)) \\ &\qquad + z_i(t-d(t)) - z_i(t) + \kappa g_i z_i(t)\big],\end{aligned} \tag{2}$$

which can be rewritten as

$$\dot{z}(t) = (\kappa\mathcal{G} - \mathcal{F}_1)z(t) + (\mathcal{F}_1 + \mathcal{F}_2)z(t-d(t)), \tag{3}$$

where

$$\begin{aligned}&z(t) = \big[z_i(t)\big]_N,\ z(t-d(t)) = \big[z_i(t-d(t))\big]_N, \\ &\mathcal{F}_1 = I\otimes F,\ \mathcal{F}_2 = \mathbf{L}\otimes F,\ \mathcal{G} = G\otimes F.\end{aligned}$$

For networked microgrids, the communication delays among different nodes usually meet some probabilistic features. The existing interval time-varying delay (ITVD) handling method in [16], [17] does not consider the delay distribution, which could lead to conservative results and degrade the voltage restoration performance. In order to fully capture the delay properties, a DDD modeling approach is employed. Then the system (3) is further expressed as

$$\begin{aligned}\dot{z}(t) = (\kappa\mathcal{G} - \mathcal{F}_1)z(t) + (\mathcal{F}_2 + \mathcal{F}_1)[\lambda(t)z(t-d_1(t)) \\ + (1-\lambda(t))z(t-d_2(t))],\end{aligned} \tag{4}$$

where $d_1(t) \in [0,\ \tau]$, $d_2(t) \in [\tau,\ d]$, $\tau \in (0,\ d)$, $\lambda(t) \in \{0,\ 1\}$ is a Bernoulli variable used to describe the probability distribution of the delay belonging to the above two intervals, and

$$\begin{aligned}&z(t-d_a(t)) = \big[z_i(t-d_a(t))\big]_N,\ a = 1, 2, \\ &\mathbb{E}\{\lambda(t)\} = \lambda_1,\ \mathbb{E}\{1-\lambda(t)\} = 1-\lambda_1 = \lambda_2.\end{aligned}$$

Remark 1: If $\tau = d$ and $\lambda_1 = 1$, the considered DDD approach is reduced to the traditional ITVD approach in [16], [17]. In addition, a more specific delay model can be derived by dividing the delay into more intervals with corresponding probabilities.

Following [19], the output of module k_{qi} and the auxiliary control of voltage $u_i(t)$ are chosen as the state variables $x_{1i}(t)$ and $x_{2i}(t)$, respectively. Specifically, $x_{1i}(t)$ means the output signal of droop control and $x_{2i}(t)$ means the output signal of secondary control. Then, the system state space form based on the small-signal model is established as

$$\begin{aligned}&\begin{bmatrix}\dot{x}_{1i}(t)\\ \dot{x}_{2i}(t)\end{bmatrix} = \begin{bmatrix}-\frac{1+\rho_{1i}k_{qi}}{t_p} & \frac{\rho_{1i}k_{qi}}{t_p}\\ 0 & 0\end{bmatrix}\begin{bmatrix}x_{1i}(t)\\ x_{2i}(t)\end{bmatrix} + \begin{bmatrix}0\\ 1\end{bmatrix}\dot{u}_i(t), \\ &y_i(t) = \begin{bmatrix}-1 & 1\end{bmatrix}\begin{bmatrix}x_{1i}(t) & x_{2i}(t)\end{bmatrix}^\top,\end{aligned} \tag{5}$$

where $y_i(t) = y_{ri}(t) - y_{mi}(t)$ means the small deviation signal between the estimated reference voltage signal $y_{ri}(t)$ and the measured voltage $y_{mi}(t)$, t_p is the time constant of low pass filter [31], $\rho_{1i} = \frac{V_e cos\phi_{ie}}{X_i}$, $\rho_{2i} = \frac{E_{ie}cos\phi_{ie} - 2V_e}{X_i}$. ΔV denotes the voltage deviation of common bus, it can be set as 0 because the common bus voltage is stable around the equilibrium point. For the calculation of plant parameters (ρ_{1i}, ρ_{2i}), the parameters are chosen the same with [31] as $E_{ie} = 1$ per unit, $V_e = 1$ per unit, $\phi_{ie} = 0$, and $X_i = 0.001$ per unit.

By considering the fact that only the output voltage is measured, a local PIO is designed to obtain the estimation of system state as

$$\begin{cases}\dot{\hat{x}}_i(t) = A_i\hat{x}_i(t) + B_i\dot{u}_i(t) \\ +H_i\big(y_i(t) - \hat{y}_i(t)\big) + W_i m_i(t)\big] \\ \hat{y}_i(t) = C\hat{x}_i(t) \\ \dot{m}_i(t) = M_i\big(y_i(t) - \hat{y}_i(t)\big),\end{cases} \tag{6}$$

in which the estimation of $x_i(t)$ is denoted by $\hat{x}_i(t)$, $m_i(t) = M_i \int (y_i(t) - \hat{y}_i(t))dt$ is the integration of output error $y_i(t) - \hat{y}_i(t)$, H_i and M_i are observer gains to be designed, W_i is a given constant matrix and

$$A_i = \begin{bmatrix} -\frac{1+\rho_{1i}k_{qi}}{t_p} & \frac{\rho_{1i}k_{qi}}{t_p} \\ 0 & 0 \end{bmatrix},\ B_i = \begin{bmatrix} 0 \\ 1 \end{bmatrix},\ C = \begin{bmatrix} -1 & 1 \end{bmatrix}.$$

Remark 2: In the considered PIO (6), an extra integral term $m_i(t) = M_i \int (y_i(t) - \hat{y}_i(t))dt$ utilizing the historical output is introduced. With the help of more information, it is potential to improve the accuracy of state estimation. When $W_i = 0$ is set, the PIO (6) reduces to the following traditional PO:

$$\begin{cases} \dot{\hat{x}}_i(t) = A_i\hat{x}_i(t) + B_i\dot{u}_i(t) + H_i\big(y_i(t) - \hat{y}_i(t)\big)\big] \\ \hat{y}_i(t) = C\hat{x}_i(t). \end{cases} \tag{7}$$

This reduction means that the PIO is more general than the traditional PO.

To restore the voltages of all DGs, the distributed cooperative controller utilizing the estimated state is constructed as

$$\begin{aligned} \dot{u}_i(t) &= K_1 \sum_{j\in N_i} a_{ij}\big[\hat{x}_j(t-d(t)) - \hat{x}_i(t)\big] + K_2\hat{x}_i(t) \\ &= K_1 \sum_{j\in N_i} a_{ij}\big[\hat{x}_j(t-d(t)) - \hat{x}_i(t-d(t)) \\ &\quad + \hat{x}_i(t-d(t)) - \hat{x}_i(t)\big] + K_2\hat{x}_i(t), \end{aligned} \tag{8}$$

which can be formed as the next compact expression:

$$\dot{u}(t) = (\mathcal{K}_1 + \mathcal{K}_3)\hat{x}(t) + (\mathcal{K}_2 + \mathcal{K}_1)\hat{x}(t-d(t)), \tag{9}$$

where

$$u(t) = \big[u_i(t)\big]_N, \hat{x}(t) = \big[\hat{x}_i(t)\big]_N, \hat{x}(t-d(t)) = \big[\hat{x}_i(t-d(t))\big]_N,$$
$$\mathcal{K}_1 = I\otimes K_1,\ \mathcal{K}_2 = \mathbf{L}\otimes K_1,\ \mathcal{K}_3 = I\otimes K_2.$$

By taking into account the probabilistic distribution of communication delay, the voltage restoration controller (9) is reformed as

$$\begin{aligned} \dot{u}(t) &= (\mathcal{K}_1 + \mathcal{K}_3)\hat{x}(t) + (\mathcal{K}_2 + \mathcal{K}_1)\big[\lambda(t)\hat{x}(t-d_1(t)) \\ &\quad + (1-\lambda(t))\hat{x}(t-d_2(t))\big], \end{aligned} \tag{10}$$

where $d_1(t) \in [0,\ \tau]$, $d_2(t) \in [\tau,\ d]$, $\tau \in (0,\ d)$ and $\hat{x}(t - d_a(t)) = \big[\hat{x}_i(t-d_a(t))\big]_N,\ a = 1, 2$.

Then, the augmented closed-loop microgrid voltage control system is deduced as

$$\begin{aligned} \dot{\phi}(t) &= \mathcal{A}\phi(t) + \mathcal{I}_1^\top(\lambda(t)B(\mathcal{K}_2 + \mathcal{K}_1)\mathcal{I}_1\phi(t-d_1(t)) \\ &\quad + \mathcal{I}_1^\top((1-\lambda(t))B(\mathcal{K}_2 + \mathcal{K}_1)\mathcal{I}_1\phi(t-d_2(t)), \end{aligned} \tag{11}$$

where

$$\begin{aligned} &\phi(t) = \begin{bmatrix} e^\top(t) & \hat{x}^\top(t) & m^\top(t) \end{bmatrix}^\top, \\ &e(t) = \big[e_i(t)\big]_N,\ e_i(t) = x_i(t) - \hat{x}_i(t), \\ &\mathcal{A} = \begin{bmatrix} A-H & 0 & -W \\ H & A + B\mathcal{K}_1 + B\mathcal{K}_3 & W \\ M & 0 & 0 \end{bmatrix}, \\ &A = diag\{A_1, A_2, \ldots, A_N\}, B = diag\{B_1, B_2, \ldots, B_N\}, \\ &\mathcal{I}_1 = \begin{bmatrix} 0 & I & 0 \end{bmatrix},\ M = diag\{M_1C, M_2C, \ldots, M_NC\}, \\ &H = diag\{H_1C, H_2C, \ldots, H_NC\}. \end{aligned}$$

Remark 3: In the existing literature [19], [20], the closed-loop voltage control system based on small-signal model is established. It is difficult for control synthesis since the presence of the constant reference signal and the control parameters are tuned manually dependent on designers' experience. However, our proposed system removes this difficulty by using the estimated reference signal. Then, the observer and controller gains can be co-designed with the system stability. It demonstrates that our method is more theoretical and practical than the manual tuning method in [19], [20].

For further proceeding, a useful technical lemma is provided as below.

Lemma 1 [32]: For given scalar $\mu \in (0, 1)$, any vector $\zeta \in \mathbb{R}^q$, and matrices $J \in \mathbb{R}^{n\times n}$, $\Im_1 \in \mathbb{R}^{n\times q}$, $\Im_2 \in \mathbb{R}^{n\times q}$, define the following function $\varepsilon(\mu, J)$:

$$\varepsilon(\mu, J) = \frac{1}{\mu}\mathbf{Sy}(J, \Im_1\zeta) + \frac{1}{1-\mu}\mathbf{Sy}(J, \Im_2\zeta). \tag{12}$$

Then, if there exists $Y \in \mathbb{R}^{n\times n}$ satisfying $\begin{bmatrix} J & Y \\ Y^\top & J \end{bmatrix} > 0$, the following inequality holds

$$\min_{\mu\in(0,1)} \varepsilon(\mu, J) \geq \mathbf{Sy}\left(\begin{bmatrix} J & Y \\ Y^\top & J \end{bmatrix}, \begin{bmatrix} \Im_1 \\ \Im_2 \end{bmatrix}\zeta\right). \tag{13}$$

III. Main Results

In this section, the stability analysis conditions for the reference voltage estimating system (3) is deduced in Theorem 1. Based on this theorem, the stability analysis and controller design conditions for the closed-loop voltage control system (11) are presented in Theorem 2 and Theorem 3, respectively.

Theorem 1: For given scalars τ, d, λ_1, the reference voltage tracking control system (3) under the controller gains F and κ is asymptotically mean square stable, if there exist matrices $P_0 > 0$, $J_l > 0$, $T_l > 0$, $\mathcal{J}_l = \begin{bmatrix} J_l & Y_l \\ Y_l^\top & J_l \end{bmatrix} > 0$, $l = 0, 1$, and matrices Y_0, Y_1 and $\mathcal{Q}_0$ such that

$$\Lambda_0 + \mathbf{He}(\mathcal{Q}_0\mathcal{U}_0) < 0, \tag{14}$$

where $d_\tau = d - \tau$ and

$$\begin{aligned} \Lambda_0 &= \mathbf{He}\Big(\mathbb{O}_2^\top P_0\mathbb{O}_1\Big) + \mathbf{Sy}(\tau J_0 + d_\tau J_1, \mathbb{O}_1) \\ &\quad + \mathbf{Sy}(T_0, \mathbb{O}_2) - \mathbf{Sy}(T_0, \mathbb{O}_4) - \frac{1}{\tau}\mathbf{Sy}(\mathcal{J}_0, \mathbf{O}_0) \\ &\quad + \mathbf{Sy}(T_1, \mathbb{O}_4) - \mathbf{Sy}(T_1, \mathbb{O}_6) - \frac{1}{d_\tau}\mathbf{Sy}(\mathcal{J}_1, \mathbf{O}_1), \\ \mathcal{U}_0 &= -\mathbb{O}_1 + (\mathcal{G} - \mathcal{F}_1)\mathbb{O}_2 + \lambda_1(\mathcal{F}_2 + \mathcal{F}_1)\mathbb{O}_3 \\ &\quad + \lambda_2(\mathcal{F}_2 + \mathcal{F}_1)\mathbb{O}_5, \\ \mathbf{O}_0 &= \begin{bmatrix} \mathbb{O}_2 - \mathbb{O}_3 \\ \mathbb{O}_3 - \mathbb{O}_4 \end{bmatrix},\ \mathbf{O}_1 = \begin{bmatrix} \mathbb{O}_4 - \mathbb{O}_5 \\ \mathbb{O}_5 - \mathbb{O}_6 \end{bmatrix}, \\ \mathbb{O}_b &\triangleq \begin{bmatrix} 0_{N,Nb} & I_N & 0_{N,N(6-b)} \end{bmatrix}, b = 1, \ldots, 6. \end{aligned}$$

Proof: We choose a Lyapunov-Krasovskii functional (LKF) as

$$\begin{aligned}V_0(t) = &\mathbf{Sy}(P_0, z(t))\\ &+\int_{t-\tau}^{t}\mathbf{Sy}(T_0, z(\theta))d\theta+\int_{-\tau}^{0}\int_{t+\theta}^{t}\mathbf{Sy}(J_0,\dot{z}(v))dvd\theta\\ &+\int_{t-d}^{t-\tau}\mathbf{Sy}(T_1, z(\theta))d\theta+\int_{-d}^{-\tau}\int_{t+\theta}^{t}\mathbf{Sy}\big(J_1,\dot{\phi}(v)\big)dvd\theta.\end{aligned} \tag{15}$$

Next, $\dot{V}_0(t)$ is computed as

$$\begin{aligned}\dot{V}_0(t) = &2z^\top(t)P_0\dot{z}(t)+\mathbf{Sy}(T_0, z(t))-\mathbf{Sy}(T_0, z(t-\tau))\\ &+\tau\mathbf{Sy}(J_0,\dot{z}(t))-\int_{t-\tau}^{t}\mathbf{Sy}(J_0,\dot{z}(\theta))d\theta\\ &+\mathbf{Sy}(T_1, z(t-\tau))-\mathbf{Sy}(T_1, z(t-d))\\ &+d_{\tau\mathbf{Sy}}(J_1,\dot{z}(t))-\int_{t-d}^{t-\tau}\mathbf{Sy}(J_1,\dot{z}(\theta))d\theta.\end{aligned} \tag{16}$$

Define

$$\begin{aligned}\xi_0(t) = &\big[\dot{z}^\top(t), z^\top(t), z^\top(t-d_1(t)), z^\top(t-\tau),\\ &z^\top(t-d_2(t)), z^\top(t-d)\big]^\top.\end{aligned} \tag{17}$$

By applying Lemma 1, it results in

$$-\int_{t-\tau}^{t}\mathbf{Sy}(J_0,\dot{z}(\theta))d\theta \le -\frac{1}{\tau}\mathbf{Sy}(\mathcal{J}_0, \zeta_0(t)), \tag{18}$$

$$-\int_{t-d}^{t-\tau}\mathbf{Sy}(J_1,\dot{z}(\theta))d\theta \le -\frac{1}{d_\tau}\mathbf{Sy}(\mathcal{J}_1, \zeta_1(t)), \tag{19}$$

where

$$\begin{aligned}\zeta_0(t) &= \begin{bmatrix}\mathbb{O}_2-\mathbb{O}_3\\ \mathbb{O}_3-\mathbb{O}_4\end{bmatrix}\xi_0(t),\ \ \zeta_1(t) = \begin{bmatrix}\mathbb{O}_4-\mathbb{O}_5\\ \mathbb{O}_5-\mathbb{O}_6\end{bmatrix}\xi_0(t),\\ \mathcal{J}_0 &= \begin{bmatrix}J_0 & Y_0\\ Y_0^\top & J_0\end{bmatrix}, \zeta_0(t) = \begin{bmatrix}z(t)-z(t-d_1(t))\\ z(t-d_1(t))-z(t-\tau)\end{bmatrix},\\ \mathcal{J}_1 &= \begin{bmatrix}J_1 & Y_1\\ Y_1^\top & J_1\end{bmatrix}, \zeta_1(t) = \begin{bmatrix}z(t-\tau)-z(t-d_2(t))\\ z(t-d_2(t))-z(t-d)\end{bmatrix}.\end{aligned}$$

Then, the condition (16) is relaxed as:

$$\dot{V}_0(t) \le \mathbf{Sy}(\Lambda_0, \xi_0(t)). \tag{20}$$

From the defined $\xi_0(t)$, the system (3) is formulated as

$$\dot{z}(t) = \mathbb{O}_1\xi_0(t),\quad z(t) = \mathbb{O}_2\xi_0(t),\ \ U_0\xi_0(t) = 0, \tag{21}$$

where

$$\begin{aligned}U_0 = &-\mathbb{O}_1+(\mathcal{G}-\mathcal{F}_1)\mathbb{O}_2+\lambda(t)(\mathcal{F}_2+\mathcal{F}_1)\mathbb{O}_3\\ &+(1-\lambda(t))(\mathcal{F}_2+\mathcal{F}_1)\mathbb{O}_5.\end{aligned}$$

Calculating the mathematical expectation of the system $U_0\xi_0(t) = 0$ leads to

$$\mathbb{E}\{U_0\xi_0(t)\} = \mathcal{U}_0\xi_0(t)\ \ = 0. \tag{22}$$

In order to ensure the mean square stability of system (3), one requires

$$\mathbf{Sy}(\Lambda_0+\mathbf{He}(\mathcal{Q}_0\mathcal{U}_0), \xi_0(t)) < 0, \tag{23}$$

where $\mathcal{Q}_0$ is a slack variable matrix.

The condition (23) is ensured by (14), which fulfills the proof. ■

Theorem 2: For given scalars τ, d, λ_1, ν_1, ν_2, the closed-loop microgrid voltage control system (11) under the controller gains K_1, K_2 and observer gains H_i, W_i, M_i, $i = 1,\ldots,N$ is asymptotically mean square stable, if Theorem 1 is satisfied and there exist matrices $P_1 > 0$, $J_l > 0$, $T_l > 0$, $\mathcal{J}_l = \begin{bmatrix}J_l & Y_l\\ Y_l^\top & J_l\end{bmatrix} > 0$, $l = 2, 3$ and matrix $\mathbf{Q}$ such that

$$\Lambda_1+\mathbf{He}(\mathcal{Q}_1\mathcal{U}_1) < 0, \tag{24}$$

where

$$\begin{aligned}\Lambda_1 = &\mathbf{He}\big(\mathbb{I}_2^\top P_1\mathbb{I}_1\big)+\mathbf{Sy}(\tau J_2+d_\tau J_3, \mathbb{I}_1)\\ &+\mathbf{Sy}(T_2,\mathbb{I}_2)-\mathbf{Sy}(T_2,\mathbb{I}_4)-\frac{1}{\tau}\mathbf{Sy}(\mathcal{J}_2,\mathbf{I}_0)\\ &+\mathbf{Sy}(T_3,\mathbb{I}_4)-\mathbf{Sy}(T_3,\mathbb{I}_6)-\frac{1}{d_\tau}\mathbf{Sy}(\mathcal{J}_3,\mathbf{I}_1),\\ \mathcal{Q}_1 = &\mathbb{I}_1^\top\mathbf{Q}+\nu\mathbb{I}_2^\top\mathbf{Q},\\ \mathcal{U}_1 = &-\mathbb{I}_1+\mathcal{A}\mathbb{I}_2+\mathcal{I}_1^\top\lambda_1 B(\mathcal{K}_2+\mathcal{K}_1)\mathcal{I}_1\mathbb{I}_3\\ &+\mathcal{I}_1^\top\lambda_2 B(\mathcal{K}_2+\mathcal{K}_1)\mathcal{I}_1\mathbb{I}_5,\\ \mathbf{I}_0 = &\begin{bmatrix}\mathbb{I}_2-\mathbb{I}_3\\ \mathbb{I}_3-\mathbb{I}_4\end{bmatrix},\ \mathbf{I}_1 = \begin{bmatrix}\mathbb{I}_4-\mathbb{I}_5\\ \mathbb{I}_5-\mathbb{I}_6\end{bmatrix},\\ \mathbb{I}_b \triangleq &\big[0_{5N,5Nb}\quad I_{5N}\quad 0_{5N,5N(6-b)}\big], b = 1,\ldots,6.\end{aligned}$$

Proof: The following LKF is selected:

$$\begin{aligned}V_1(t) = &\mathbf{Sy}(P_1, \phi(t))\\ &+\int_{t-\tau}^{t}\mathbf{Sy}(T_2, \phi(\theta))d\theta+\int_{-\tau}^{0}\int_{t+\theta}^{t}\mathbf{Sy}\big(J_2,\dot{\phi}(v)\big)dvd\theta\\ &+\int_{t-d}^{t-\tau}\mathbf{Sy}(T_3, \phi(\theta))d\theta+\int_{-d}^{-\tau}\int_{t+\theta}^{t}\mathbf{Sy}\big(J_3,\dot{\phi}(v)\big)dvd\theta.\end{aligned} \tag{25}$$

We calculate $\dot{V}_1(t)$ as

$$\begin{aligned}\dot{V}_1(t) = &2\phi^\top(t)P_1\dot{\phi}(t)+\mathbf{Sy}(T_2, \phi(t))-\mathbf{Sy}(T_2, \phi(t-\tau))\\ &+\tau\mathbf{Sy}\big(J_2,\dot{\phi}(t)\big)-\int_{t-\tau}^{t}\mathbf{Sy}\big(J_2,\dot{\phi}(\theta)\big)d\theta\\ &+\mathbf{Sy}(T_3, \phi(t-\tau))-\mathbf{Sy}(T_3, \phi(t-d))\\ &+d_{\tau\mathbf{Sy}}\big(J_3,\dot{\phi}(t)\big)-\int_{t-d}^{t-\tau}\mathbf{Sy}\big(J_3,\dot{\phi}(\theta)\big)d\theta.\end{aligned} \tag{26}$$

The augmented vector $\xi_1(t)$ is defined as:

$$\begin{aligned}\xi_1(t) = &\big[\dot{\phi}^\top(t), \phi^\top(t), \phi^\top(t-d_1(t)), \phi^\top(t-\tau),\\ &\phi^\top(t-d_2(t)), \phi^\top(t-d)\big]^\top.\end{aligned} \tag{27}$$

By applying Lemma 1, it results in

$$-\int_{t-\tau}^{t}\mathbf{Sy}\big(J_2,\dot{\phi}(\theta)\big)d\theta \le -\frac{1}{\tau}\mathbf{Sy}(\mathcal{J}_2, \zeta_2(t)), \tag{28}$$

$$-\int_{t-d}^{t-\tau}\mathbf{Sy}\big(J_3,\dot{\phi}(\theta)\big)d\theta \le -\frac{1}{d_\tau}\mathbf{Sy}(\mathcal{J}_3, \zeta_3(t)), \tag{29}$$

where

$$\begin{aligned}\mathcal{J}_2 &= \begin{bmatrix}J_2 & Y_2\\ Y_2^\top & J_2\end{bmatrix}, \zeta_2(t) = \begin{bmatrix}\phi(t)-\phi(t-d_1(t))\\ \phi(t-d_1(t))-\phi(t-\tau)\end{bmatrix},\\ \mathcal{J}_3 &= \begin{bmatrix}J_3 & Y_3\\ Y_3^\top & J_3\end{bmatrix}, \zeta_3(t) = \begin{bmatrix}\phi(t-\tau)-\phi(t-d_2(t))\\ \phi(t-d_2(t))-\phi(t-d)\end{bmatrix},\\ \zeta_2(t) &= \begin{bmatrix}\mathbb{I}_2-\mathbb{I}_3\\ \mathbb{I}_3-\mathbb{I}_4\end{bmatrix}\xi_1(t),\ \ \zeta_3(t) = \begin{bmatrix}\mathbb{I}_4-\mathbb{I}_5\\ \mathbb{I}_5-\mathbb{I}_6\end{bmatrix}\xi_1(t).\end{aligned}$$

By taking the same processes in the proof of Theorem 1, the system stability in mean square sense is satisfied if

$$\mathbf{Sy}(\Lambda_1 + \mathbf{He}(\mathcal{Q}_1\mathcal{U}_1), \xi_1(t)) < 0 \tag{30}$$

holds.

It is ensured by (24) for $\mathcal{Q}_1 = \mathbb{I}_1^{\top\mathbf{Q}} + \nu\mathbb{I}_2^{\top\mathbf{Q}}$. Then the proof is completed. ■

Theorem 3: For given scalars τ, d, λ_1, ν, σ, the closed-loop microgrid voltage control system (11) is asymptotically mean square stable, if Theorem 1 is satisfied and there exist matrices $\hat{P}_1 > 0$, $\hat{J}_l > 0$, $\hat{T}_l > 0$, $\hat{\mathcal{J}}_l = \begin{bmatrix} \hat{J}_l & \hat{Y}_l \\ \hat{Y}_l^\top & \hat{J}_l \end{bmatrix} > 0$, $l = 2, 3$ and matrices R_{K1}, R_{K2}, R_{Hi}, R_{Wi}, S_i, $i = 1, \ldots, N$, $\mathbf{X} = \begin{bmatrix} X_1 & 0 & X_1 Z \\ 0 & X_2 & 0 \\ Z^\top X_1 & 0 & X_3 \end{bmatrix}$ such that

$$\hat{\Lambda}_1 + \mathbf{He}\left(\hat{\mathcal{Q}}_1\hat{\mathcal{U}}_1\right) < 0, \tag{31}$$

$$\begin{bmatrix} -\sigma I & * \\ (I_N \otimes C)X_1 - S(I_N \otimes C) & -I \end{bmatrix} < 0, \tag{32}$$

where $d_\tau = d - \tau$ and

$$\begin{aligned}
\hat{\Lambda}_1 =\ & \mathbf{He}(\mathbb{I}_2^\top \hat{P}_1 \mathbb{I}_1) + \mathbf{Sy}\left(\tau\hat{J}_2 + d_\tau\hat{J}_3, \mathbb{I}_1\right) \\
& + \mathbf{Sy}\left(\hat{T}_2, \mathbb{I}_2\right) - \mathbf{Sy}\left(\hat{T}_2, \mathbb{I}_4\right) - \frac{1}{\tau}\mathbf{Sy}\left(\hat{\mathcal{J}}_2, \mathbf{I}_2\right) \\
& + \mathbf{Sy}\left(\hat{T}_3, \mathbb{I}_4\right) - \mathbf{Sy}\left(\hat{T}_3, \mathbb{I}_6\right) - \frac{1}{d_\tau}\mathbf{Sy}\left(\hat{\mathcal{J}}_3, \mathbf{I}_3\right), \\
\hat{\mathcal{Q}}_1 =\ & \mathbb{I}_1^\top + \nu\mathbb{I}_2^\top, \\
\hat{\mathcal{U}}_1 =\ & -X_1\mathbb{I}_1 + \hat{\mathcal{A}}\mathbb{I}_2 + \mathcal{I}^\top\lambda_1 B\left(\hat{\mathcal{K}}_2 + \hat{\mathcal{K}}_1\right)\mathcal{I}\mathbb{I}_3 \\
& + \mathcal{I}^\top\lambda_2 B\left(\hat{\mathcal{K}}_2 + \hat{\mathcal{K}}_1\right)\mathcal{I}\mathbb{I}_5, \\
\hat{\mathcal{A}} =\ & \begin{bmatrix} \hat{\mathcal{A}}_{11} & 0 & \hat{\mathcal{A}}_{13} \\ R_H + WZ^\top X_1 & \hat{\mathcal{A}}_{22} & R_H Z + WX_3 \\ R_M & 0 & R_M Z \end{bmatrix}, \\
\hat{\mathcal{A}}_{11} =\ & AX_1 - R_H - WZ^\top X_1, \ \hat{\mathcal{K}}_1 = I_N \otimes R_{K1}, \\
\hat{\mathcal{A}}_{13} =\ & AX_1 Z - R_H Z - WX_3, \ \hat{\mathcal{K}}_2 = L \otimes R_{K1}, \\
\hat{\mathcal{A}}_{22} =\ & AX_2 + B\left(\hat{\mathcal{K}}_1 + \hat{\mathcal{K}}_3\right), \ \hat{\mathcal{K}}_3 = I_N \otimes R_{K2}.
\end{aligned}$$

Then, the controller and observer gains can be solved by

$$\begin{aligned}
K_1 = R_{K1}\bar{X}_2^{-1}, K_2 = R_{K2}\bar{X}_2^{-1}, \\
H_i = R_{Hi}S_i^{-1}, M_i = R_{Mi}S_i^{-1}.
\end{aligned}$$

Proof: Define

$$\begin{aligned}
\mathbf{Q}^{-1} = \mathbf{X} = \begin{bmatrix} X_1 & 0 & X_1 Z \\ 0 & X_2 & 0 \\ Z^\top X_1^\top & 0 & X_3 \end{bmatrix}, X_j = I_N \otimes \bar{X}_j, j = 1, 2, \\
\hat{P}_1 = \mathbf{X}P_1\mathbf{X}, \hat{J}_l = \mathbf{X}J_l\mathbf{X}, \hat{T}_l = \mathbf{X}T_l\mathbf{X}, \hat{Y}_l = \mathbf{X}Y_l\mathbf{X}, \ l = 2, 3, \\
R_{K1} = K_1\bar{X}_2, R_{K2} = K_2\bar{X}_2, R_{Hi} = H_iS_i, R_{Mi} = M_iS_i, \\
R_H = diag\{R_{H1}C, \ldots, R_{HN}C\}, S = diag\{S_1, \ldots, S_N\}, \\
R_M = diag\{R_{M1}C, \ldots, R_{MN}C\}, \\
(I_N \otimes C)X_1 = S(I_N \otimes C).
\end{aligned} \tag{33}$$

By left-and right-multiplying the condition (24) by matrix $\mathbb{X} = diag\{\mathbf{X}, \mathbf{X}, \mathbf{X}, \mathbf{X}, \mathbf{X}, \mathbf{X}\}$ and its transpose, it leads to

$$\hat{\Lambda}_1 + \mathbf{He}\left(\hat{\mathcal{Q}}_1\tilde{\mathcal{U}}_1\right) < 0, \tag{34}$$

where

$$\begin{aligned}
\tilde{\mathcal{U}}_1 =\ & -X_1\mathbb{I}_1 + \tilde{\mathcal{A}}\mathbb{I}_2 + \mathcal{I}_1^\top\lambda_1 B\left(\tilde{\mathcal{K}}_2 + \tilde{\mathcal{K}}_1\right)\mathcal{I}_1\mathbb{I}_3 \\
& + \mathcal{I}_1^\top\lambda_2 B\left(\tilde{\mathcal{K}}_2 + \tilde{\mathcal{K}}_1\right)\mathcal{I}_1\mathbb{I}_5, \\
\tilde{\mathcal{A}} =\ & \begin{bmatrix} \tilde{\mathcal{A}}_{11} & 0 & \tilde{\mathcal{A}}_{13} \\ HX_1 + WZ^\top X_1 & \tilde{\mathcal{A}}_{22} & HX_1 Z + WX_3 \\ MX_1 & 0 & MX_1 Z \end{bmatrix}, \\
\tilde{\mathcal{A}}_{11} =\ & AX_1 - HX_1 - WZ^\top X_1, \\
\tilde{\mathcal{A}}_{13} =\ & AX_1 Z - HX_1 Z - WX_3, \\
\tilde{\mathcal{A}}_{22} =\ & AX_2 + B\mathcal{K}_1 X_2 + B\mathcal{K}_3 X_2, \\
\tilde{\mathcal{K}}_1 =\ & \mathcal{K}_1 X_2, \ \tilde{\mathcal{K}}_2 = \mathcal{K}_2 X_2.
\end{aligned}$$

It is equivalent to the condition (31) according to the definitions in (33).

The equation constraint $(I_N \otimes C)X_1 = S(I_N \otimes C)$ can be expressed as

$$\mathbf{Sy}(I, (I_N \otimes C)X_1 - S(I_N \otimes C)) = 0. \tag{35}$$

By exploiting Schur complement to (35), it is converted as the optimization condition (32), which fulfills the proof. ■

If the traditional PO (7) is considered, the corresponding closed-loop system is formulated as:

$$\begin{aligned}
\dot{\phi}(t) = \mathcal{A}\phi(t) + \mathcal{I}_1^\top(\lambda(t)B(\mathcal{K}_2 + \mathcal{K}_1)\mathcal{I}_1\phi(t - d_1(t)) \\
+ \mathcal{I}_1^\top((1 - \lambda(t))B(\mathcal{K}_2 + \mathcal{K}_1)\mathcal{I}_1\phi(t - d_2(t)),
\end{aligned} \tag{36}$$

where

$$\begin{aligned}
\phi(t) = \begin{bmatrix} e^\top(t) & \hat{x}^\top(t) \end{bmatrix}^\top, \ \mathcal{I}_1 = \begin{bmatrix} 0 & I \end{bmatrix}, \\
\mathcal{A} = \begin{bmatrix} A - H & 0 \\ H & A + B\mathcal{K}_1 + B\mathcal{K}_3 \end{bmatrix}.
\end{aligned}$$

Then, the co-design conditions are attained in the following corollary by the same method used in Theorem 3.

Corollary 1: For given τ, d, λ_1, λ_2, ν, the system (9) under the conventional PO (7) and controller (9) is asymptotically mean square stable, if there exist matrices $\hat{P}_1 > 0$, $\hat{J}_l > 0$, $\hat{T}_l > 0$, $\hat{\mathcal{J}}_l = \begin{bmatrix} \hat{J}_l & \hat{Y}_l \\ \hat{Y}_l^\top & \hat{J}_l \end{bmatrix} > 0$, $l = 2, 3$ and matrices R_{K1}, R_{K2}, R_{Hi}, R_{Wi}, S_i, $i = 1, \ldots, N$, $\mathbf{X} = \begin{bmatrix} X_1 & 0 \\ 0 & X_2 \end{bmatrix}$ such that

$$\hat{\Lambda}_1 + \mathbf{He}\left(\hat{\mathcal{Q}}_1\hat{\mathcal{U}}_1\right) < 0, \tag{37}$$

$$\begin{bmatrix} -\sigma I & * \\ (I_N \otimes C)X_1 - S(I_N \otimes C) & -I \end{bmatrix} < 0 \tag{38}$$

where

$$\begin{aligned}
\hat{\Lambda}_1 =\ & \mathbf{He}(\mathbb{I}_2^\top \hat{P}_1 \mathbb{I}_1) + \mathbf{Sy}\left(\tau\hat{J}_2 + d_\tau\hat{J}_3, \mathbb{I}_1\right) + \mathbf{Sy}\left(\hat{T}_2, \mathbb{I}_2\right) \\
& - \mathbf{Sy}\left(\hat{T}_2, \mathbb{I}_4\right) + \mathbf{Sy}\left(\hat{T}_3, \mathbb{I}_4\right) - \mathbf{Sy}\left(\hat{T}_3, \mathbb{I}_6\right) \\
& - \frac{1}{\tau}\mathbf{Sy}\left(\hat{\mathcal{J}}_2, \mathbf{I}_2\right) - \frac{1}{d_\tau}\mathbf{Sy}\left(\hat{\mathcal{J}}_3, \mathbf{I}_3\right),
\end{aligned}$$

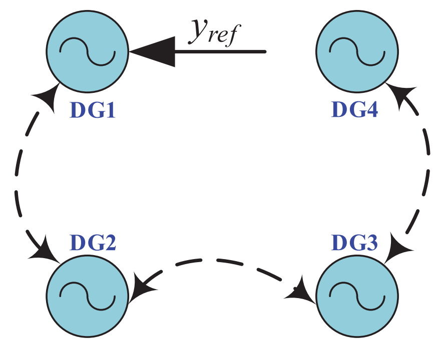

Fig. 2. The communication graph topology.

$$\begin{aligned}
\hat{\mathcal{Q}}_1 &= \mathbb{I}_1^\top + \nu \mathbb{I}_2^\top,\\
\hat{\mathcal{U}}_1 &= -X_1\mathbb{I}_1 + \hat{\mathcal{A}}\mathbb{I}_2 + \mathcal{I}^\top\lambda_1 B\Big(\hat{\mathcal{K}}_2 + \hat{\mathcal{K}}_1\Big)\mathcal{I}\mathbb{I}_3\\
&\quad + \mathcal{I}^\top\lambda_2 B\Big(\hat{\mathcal{K}}_2 + \hat{\mathcal{K}}_1\Big)\mathcal{I}\mathbb{I}_5,\\
\hat{\mathcal{A}} &= \begin{bmatrix} \hat{\mathcal{A}}_{11} & 0 \\ R_H + WZ^\top X_1 & \hat{\mathcal{A}}_{22}\end{bmatrix},\\
\hat{\mathcal{A}}_{11} &= AX_1 - R_H - WZ^\top X_1,\ \hat{\mathcal{A}}_{22} = AX_2 + B\Big(\hat{\mathcal{K}}_1 + \hat{\mathcal{K}}_3\Big),\\
\hat{\mathcal{K}}_1 &= I_N \otimes R_{K1},\ \ \hat{\mathcal{K}}_2 = L \otimes R_{K1},\ \ \hat{\mathcal{K}}_3 = I_N \otimes R_{K2},\\
\mathbb{I}_b &\triangleq \begin{bmatrix} 0_{4N,4Nb} & I_{4N} & 0_{4N,4N(6-b)}\end{bmatrix}, b = 1, \ldots, 6.
\end{aligned}$$

Then, the controller and observer gains are computed by $K_1 = R_{K1}\bar{X}_2^{-1}$, $K_2 = R_{K2}\bar{X}_2^{-1}$, $H_i = R_{Hi}S_i^{-1}$, $M_i = R_{Mi}S_i^{-1}$.

IV. Simulation Results

In the simulation, a networked microgrid with four inverter-based DGs is introduced to verify the benefits of the presented distributed cooperative voltage control mechanism. The communication links among DGs are drawn in Fig. 2, which indicates that the reference signal $y_{ref} = 311V$ is only available for DG1 and $G = diag\{1, 0, 0, 0\}$. The associated adjacency matrix and Laplacian matrix are given as:

$$\mathbf{A} = \begin{bmatrix} 0 & 1 & 0 & 0\\ 1 & 0 & 1 & 0\\ 0 & 1 & 0 & 1\\ 0 & 0 & 1 & 0\end{bmatrix}, \mathbf{L} = \begin{bmatrix} 1 & -1 & 0 & 0\\ -1 & 2 & -1 & 0\\ 0 & -1 & 2 & -1\\ 0 & 0 & -1 & 1\end{bmatrix}.$$

The considered probabilistic communication delay with upper bound $d = 0.015s$ and its cumulative probability are drawn in Fig. 3. According to this figure, the delay distribution information can be obtained as $\tau = 0.01s$, $\lambda_1 = 0.6$ and $\lambda_2 = 0.4$. It means the probability of $d(t) \in [0,\ \tau]$ is 0.6 and the probability of $d(t) \in (\tau,\ d]$ is 0.4. The other parameters are chosen as $\nu = 1$, $F = -20$, $\kappa = 50$ and

$$W_1 = W_2 = W_3 = W_4 = \begin{bmatrix} 1 \\ -0.1\end{bmatrix},$$
$$Z_1 = Z_2 = Z_3 = Z_4 = \begin{bmatrix} 0 \\ 10\end{bmatrix}.$$

The system parameters are selected as $t_p = 0.001$, $k_{q1} = k_{q2} = 0.9 \times 10^{-3}$ and $k_{q3} = k_{q4} = 1.19 \times 10^{-3}$. By solving the conditions in Theorem 3, the gains of controllers and observers are shown as

$$\begin{aligned}
K_1 &= \begin{bmatrix}-0.5570\ 0.9948\end{bmatrix},\\
K_2 &= 10^3 \times \begin{bmatrix}0.8137\ -2.1913\end{bmatrix},\\
H_1 &= \begin{bmatrix}-17.6949\\ 26.0015\end{bmatrix},\ H_2 = \begin{bmatrix}-17.6940\\ 25.9986\end{bmatrix},\\
H_3 &= \begin{bmatrix}-16.8566\\ 31.7877\end{bmatrix},\ H_4 = \begin{bmatrix}-16.8828\\ 31.7926\end{bmatrix},\\
M_1 &= -181.2876,\ M_2 = -181.2903,\\
M_3 &= -220.5870,\ M_4 = -220.5968.
\end{aligned}$$

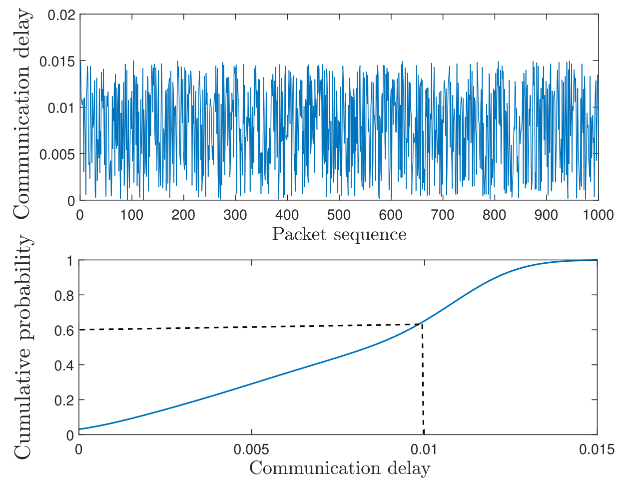

Fig. 3. Probabilistic communication delay and its cumulative probability.

In simulation, we consider the simulation step as $10^{-4}s$. Fig. 4 shows the open-loop voltage responses of all DGs, which can not be restored to reference voltage without secondary control. The estimated reference voltage signals and the measured voltage signals are illustrated in Fig. 5 and Fig. 6, respectively. These figures show that the solved controller and observer gains can guarantee the voltages of all DGs to be tracked well to the reference signal under the islanded operation mode.

A. Plug-and-Play Test

To show the plug-and-play capability of the DG unit, DG4 is firstly disconnected from the microgrid at $t = 3.5s$, which means the communication link between DG4 and DG3 is deleted in the simulation. Next, DG4 is plugged in the microgrid at $t = 6s$, which means the communication link between DG4 and DG3 is recovered. The same parameters with the above simulation are utilized. The voltage responses of all DGs for plug-and-play test are drawn in Fig. 7. From this figure, it is seen that the proposed distributed secondary control strategy can effectively maintain the microgrid voltages at the reference value when DG4 is plugged in and removed from the microgrid.

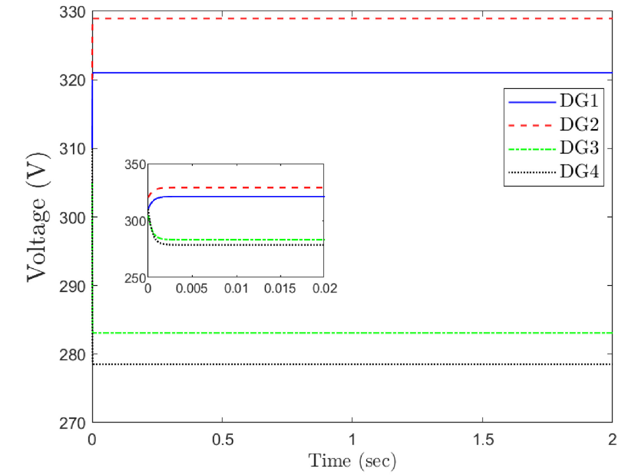

Fig. 4. The measured voltage signals $y_{mi}(t)$ for all DGs without secondary control.

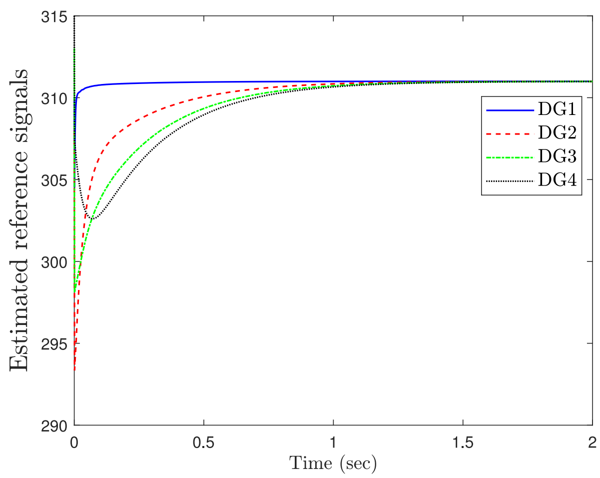

Fig. 5. The estimated reference signals $y_{ri}(t)$ of all DGs with secondary control.

B. The Effect of Probabilistic Time-Varying Delays on Control Performance

Three upper bounds of the delay: $d = 0.015s$, $d = 0.03s$ and $d = 0.045s$ are considered. In addition, the probability distributions of the three communication delay cases are $\tau = 0.01s$, $\lambda_1 = 0.6$ and $\lambda_2 = 0.4$. The other parameters are the same with the above simulation.

The curves of the voltages obtained by our PIO method for different delay cases are drawn in Fig. 8. This figure illustrates that as the increase of the delay upper bound, the convergence time and overshoot amplitude are enlarged, which implies that the control performance are degraded.

C. The Comparison of PIO and PO

Based on the same parameters considered in the above simulation, the corresponding gains of controllers and observers solved by Corollary 1 are given as:

$$K_1 = \begin{bmatrix}-0.4210 & 0.4410\end{bmatrix}, K_2 = 10^3 \times \begin{bmatrix}1.0303 & -2.3332\end{bmatrix},$$

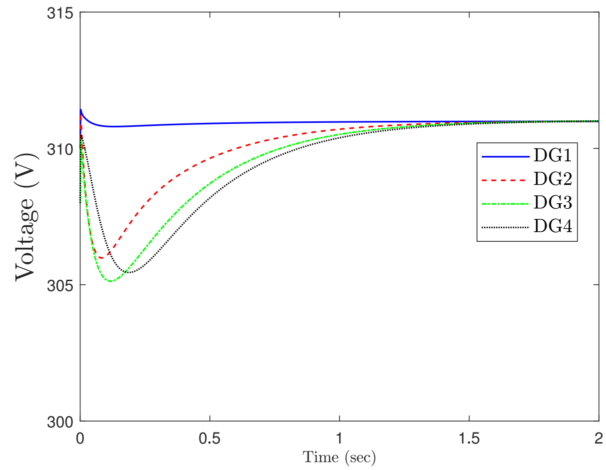

Fig. 6. The measured voltage signals $y_{mi}(t)$ for all DGs with secondary control.

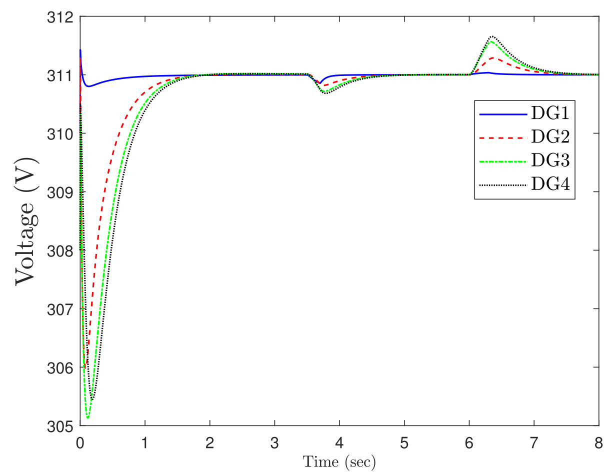

Fig. 7. The voltage evolution processes for plug-and-play feature with secondary control.

$$H_1 = \begin{bmatrix}27.4407\\58.1383\end{bmatrix}, H_2 = \begin{bmatrix}27.5959\\58.2521\end{bmatrix},$$
$$H_3 = \begin{bmatrix}31.8663\\67.2644\end{bmatrix}, H_4 = \begin{bmatrix}31.7332\\67.0435\end{bmatrix}.$$

The responses of observation error obtained by our proposed PIO and the conventional PO are compared in Fig. 9 and Fig. 10. It is seen from these figures that the estimation accuracy between the system state $x_i(t)$ and observer state $\hat{x}_i(t)$ is improved dramatically by our PIO compared to the conventional PO.

D. The Comparison of DDD and Conventional ITVD

To show the merit of the DDD method, TABLE I gives the maximum delay upper bound d obtained by our method and the conventional ITVD method. In terms of this table, it is apparently that larger d is derived via the considered DDD method (4) than the traditional ITVD method. Specifically, the maximum d is enlarged by 111.9% ($\lambda_1 = 0.8$), 27.4%

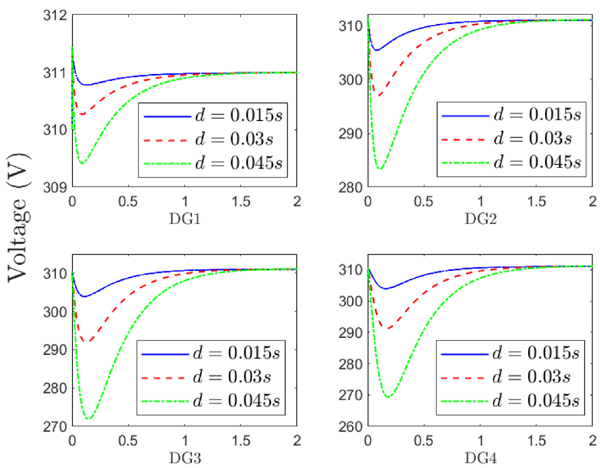

Fig. 8. Measured voltage signals $y_{mi}(t)$ for different delays.

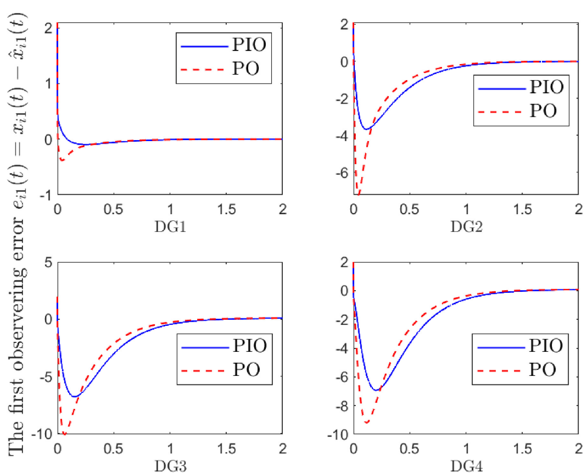

Fig. 9. The first error $e_{i1}(t)$ for different observers.

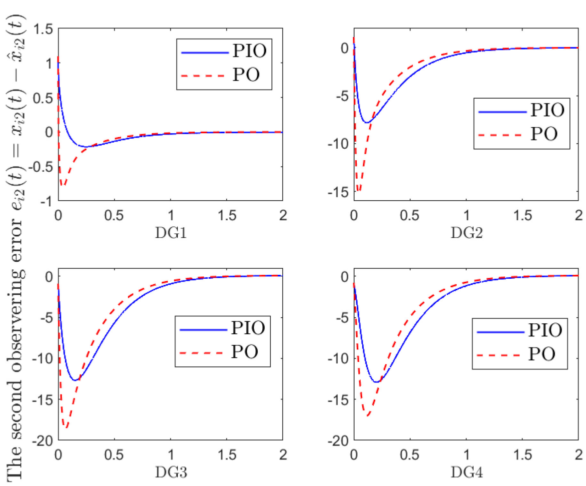

Fig. 10. The second error $e_{i2}(t)$ for different observers.

($\lambda_1 = 0.5$) and 10.3% ($\lambda_1 = 0.2$) compared to the ITVD method (3), respectively. This indicates that the delay distribution introduced in our DDD method is capable of yielding less conservative results.

TABLE I
THE MAXIMUM DELAY UPPER BOUND d UNDER DIFFERENT METHODS FOR $F = -24$ AND $\kappa = 50$

Methods	$d(s)$
DDD method with $\tau = 0.01s$, $\lambda_1 = 0.8$	0.0248
DDD method with $\tau = 0.01s$, $\lambda_1 = 0.5$	0.0149
DDD method with $\tau = 0.01s$, $\lambda_1 = 0.2$	0.0129
Conventional ITVD method	0.0117

V. CONCLUSION

The distributed cooperative voltage control problem of networked microgrids under probabilistic transmission delays has been investigated in this paper. In order to overcome the difficulty of controller design based on the existing small-signal system model with a constant reference signal, a distributed control law was constructed to obtain the estimation of reference signal for all DGs. Consequently, a new small-signal model was established by using the deviation between the estimated and measured voltages as the small signal. To handle the probabilistic communication delay, a DDD approach considering its stochastic feature was applied. A PIO based on the local measured output was adopted to derive more accurate estimation of the system state. According to these strategies, sufficient LMI conditions were deduced to co-design the controller and observer gains, which can ensure all DGs track the reference voltage well. At last, the advantages of the presented method were demonstrated by some comparison simulations.

Recently, a useful average voltage restoration strategy based on PI-consensus distributed control is proposed for islanded AC microgrids [23] and modular multilevel converter-based multi-terminal high-voltage direct current systems [33], respectively. This control strategy is able to overcome the difficulty of balancing the accurate voltage regulation and reactive power sharing due to line impedances. In terms of this advantage, it will be considered and utilized in our future research. Additionally, how to extend the proposed voltage control strategy to microgrids with cyber-attacks [34], [35] is another interesting topic and deserves further investigation.

REFERENCES

[1] X. Tang, X. Hu, N. Li, W. Deng, and G. Zhang, "A novel frequency and voltage control method for islanded microgrid based on multienergy storages," *IEEE Trans. Smart Grid*, vol. 7, no. 1, pp. 410–419, Jan. 2018.
[2] X. Liu, C. Wen, Q. Xu, and Y. Wang, "Resilient control and analysis for DC microgrid system under DoS and impulsive FDI attacks," *IEEE Trans. Smart Grid*, vol. 12, no. 5, pp. 3742–3754, Sep. 2021.
[3] T. Qian, Y. Liu, W. Zhang, W. Tang, and M. Shahidehpour, "Event-triggered updating method in centralized and distributed secondary controls for islanded microgrid restoration," *IEEE Trans. Smart Grid*, vol. 11, no. 2, pp. 1387–1395, Mar. 2020.
[4] S. Yan, Z. Gu, J. H. Park, X. Xie, and C. Dou, "Probability-density-dependent load frequency control of power systems with random delays and cyber-attacks via circuital implementation," *IEEE Trans. Smart Grid*, vol. 13, no. 6, pp. 4837–4847, Nov. 2022.
[5] F. Yang, J. He, and Q. Pan, "Further improvement on delay-dependent load frequency control of power systems via truncated B–L inequality," *IEEE Trans. Power Syst.*, vol. 33, no. 5, pp. 5062–5071, Sep. 2018.
[6] M. Zhang, S. Dong, P. Shi, G. Chen, and X. Guan, "Distributed observer-based event-triggered load frequency control of multiarea power systems under cyber attacks," *IEEE Trans. Autom. Sci. Eng.*, vol. 20, no. 4, pp. 2435–2444, Oct. 2023, doi: 10.1109/TASE.2022.3208016.

[7] K. Lu and Z. Wu, "Resilient event-triggered load frequency control for cyber-physical power systems under DoS attacks," *IEEE Trans. Power Syst.*, vol. 38, no. 6, pp. 5302–5313, Nov. 2023.
[8] M. M. Hossain, C. Peng, H. Sun, and S. Xie, "Bandwidth allocation-based distributed event-triggered LFC for smart grids under hybrid attacks," *IEEE Trans. Smart Grid*, vol. 13, no. 1, pp. 820–830, Jan. 2022.
[9] Q. Zhou, Z. Tian, M. Shahidehpour, X. Liu, A. Alabdulwahab, and A. Abusorrah, "Optimal consensus-based distributed control strategy for coordinated operation of networked microgrids," *IEEE Trans. Power Syst.*, vol. 35, no. 3, pp. 2452–2462, May 2020.
[10] N. M. Dehkordi, N. Sadati, and M. Hamzeh, "Fully distributed cooperative secondary frequency and voltage control of islanded microgrids," *IEEE Trans. Energy Convers.*, vol. 32, no. 2, pp. 675–685, Jun. 2017.
[11] G. Lou, W. Gu, Y. Xu, M. Cheng, and W. Liu, "Distributed MPC-based secondary voltage control scheme for autonomous droop-controlled microgrids," *IEEE Trans. Sustain. Energy*, vol. 8, no. 2, pp. 792–804, Apr. 2017.
[12] C. Deng, W. Che, and Z. Wu, "A dynamic periodic event-triggered approach to consensus of heterogeneous linear multiagent systems with time-varying communication delays," *IEEE Trans. Cybern.*, vol. 51, no. 4, pp. 1812–1821, Apr. 2021.
[13] B. Wei, F. Xiao, F. Fang, and Y. Shi, "Velocity-free event-triggered control for multiple Euler–Lagrange systems with communication time delays," *IEEE Trans. Autom. Control*, vol. 66, no. 11, pp. 5599–5605, Nov. 2021.
[14] K. Li, C. Hua, X. You, and X. Guan, "Finite-time observer-based leader-following consensus for nonlinear multiagent systems with input delays," *IEEE Trans. Cybern.*, vol. 51, no. 12, pp. 5850–5858, Dec. 2021.
[15] L. Ding, Q.-L. Han, L. Wang, and E. Sindi, "Distributed cooperative optimal control of DC microgrids with communication delays," *IEEE Trans. Ind. Informat.*, vol. 14, no. 9, pp. 3924–3935, Sep. 2018.
[16] C. Dou, Y. Dong, Z. Zhang, and K. Ma, "MAS-based distributed cooperative control for DC microgrid through switching topology communication network with time-varying delays," *IEEE Syst. J.*, vol. 13, no. 1, pp. 615–624, Mar. 2019.
[17] J. Lai, H. Zhou, X. Lu, X. Yu, and W. Hu, "Droop-based distributed cooperative control for microgrids with time-varying delays," *IEEE Trans. Smart Grid*, vol. 7, no. 4, pp. 1775–1789, Jul. 2016.
[18] S. Yan, Z. Gu, J. H. Park, and X. Xie, "A delay-kernel-dependent approach to saturated control of linear systems with mixed delays," *Automatica*, vol. 152, Jun. 2023, Art. no. 110984.
[19] C. Zhao, W. Sun, J. Wang, Q. Li, D. Mu, and X. Xu, "Distributed cooperative secondary control for islanded microgrid with Markov time-varying delays," *IEEE Trans. Energy Convers.*, vol. 34, no. 4, pp. 2235–2247, Dec. 2019.
[20] W. Sun, L. Huang, Z. Liu, Q. Li, C. Zhao, and D. Mu, "Distributed controller design and stability criterion for microgrids with time-varying delay and rapid switching communication topology," *Sustain. Energy, Grids Netw.*, vol. 29, Mar. 2022, Art. no. 100566.
[21] X. Li et al., "Observer-based DC voltage droop and current feed-forward control of a DC microgrid," *IEEE Trans. Smart Grid*, vol. 9, no. 5, pp. 5207–5216, Sep. 2018.
[22] R. Lu, J. Wang, and Z. Wang, "Distributed observer-based finite-time control of AC microgrid under attack," *IEEE Trans. Smart Grid*, vol. 12, no. 1, pp. 157–168, Jan. 2021.
[23] M. Shi, X. Chen, M. Shahidehpour, Q. Zhou, and J. Wen, "Observer-based resilient integrated distributed control against cyberattacks on sensors and actuators in islanded AC microgrids," *IEEE Trans. Smart Grid*, vol. 12, no. 3, pp. 1953–1963, May 2021.
[24] M. Mola, A. Afshar, N. Meskin, and M. Karrari, "Distributed fast fault detection in DC microgrids," *IEEE Syst. J.*, vol. 16, no. 1, pp. 440–451, Mar. 2022.
[25] M. R. Khalghani, J. Solanki, S. K. Solanki, M. H. Khooban, and A. Sargolzaei, "Resilient frequency control design for microgrids under false data injection," *IEEE Trans. Ind. Electron.*, vol. 68, no. 3, pp. 2151–2162, Mar. 2021.
[26] M. Wu, F. Gao, P. Yu, J. She, and W. Cao, "Improve disturbance-rejection performance for an equivalent-input-disturbance-based control system by incorporating a proportional-integral observer," *IEEE Trans. Ind. Electron.*, vol. 67, no. 2, pp. 1254–1260, Feb. 2020.
[27] J. Cheng, L. Liang, H. Yan, J. Cao, S. Tang, and K. Shi, "Proportional-integral observer-based state estimation for Markov memristive neural networks with sensor saturations," *IEEE Trans. Neural Netw. Learn. Syst.*, vol. 35, no. 1, pp. 405–416, Jan. 2024.
[28] M. Shen, T. Zhang, J. H. Park, Q. G. Wang, and L. Li, "Iterative proportional-integral interval estimation of linear discrete-time systems," *IEEE Trans. Autom. Control*, vol. 68, no. 7, pp. 4249–4256, Jul. 2023, doi: 10.1109/TAC.2022.3203226.
[29] H. Yan, C. Hu, H. Zhang, H. R. Karimi, X. Jiang, and M. Liu, "H_∞ output tracking control for networked systems with adaptively adjusted event-triggered scheme," *IEEE Trans. Syst., Man, Cybern., Syst.*, vol. 49, no. 10, pp. 2050–2058, Oct. 2019.
[30] C. Peng and J. Zhang, "Delay-distribution-dependent load frequency control of power systems with probabilistic interval delays," *IEEE Trans. Power Syst.*, vol. 31, no. 4, pp. 3309–3317, Jul. 2016.
[31] Q. Shafiee, Č. Stefanović, T. Dragičević, P. Popovski, J. C. Vasquez, and J. M. Guerrero, "Robust networked control scheme for distributed secondary control of islanded microgrids," *IEEE Trans. Ind. Electron.*, vol. 61, no. 10, pp. 5363–5374, Oct. 2013.
[32] P. Park, J. W. Ko, and C. Jeong, "Reciprocally convex approach to stability of systems with time-varying delays," *Automatica*, vol. 47, no. 1, pp. 235–238, 2011.
[33] Q. Yang, Y. Chen, Y. Lin, X. Chen, and J. Wen, "PI consensus-based integrated distributed control of MMC-MTDC systems," *IEEE Trans. Power Syst.*, vol. 38, no. 3, pp. 2333–2347, May 2023.
[34] H. Yang, C. Peng, and Z. Cao, "Attack-model-independent stabilization of networked control systems under a jump-like TOD scheduling protocol," *Automatica*, vol. 152, Jun. 2023, Art. no. 110982.
[35] Y. Zhang, C. Peng, C. Cheng, and Y. Wang, "Attack intensity dependent adaptive load frequency control of interconnected power systems under malicious traffic attacks," *IEEE Trans. Smart Grid*, vol. 14, no. 2, pp. 1223–1235, Mar. 2023.

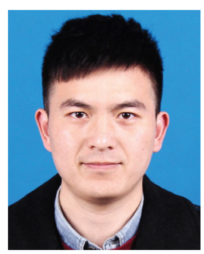

Shen Yan received the B.E. degree in automation and Ph.D. degree in power engineering automation from Nanjing Technology University, Nanjing, China, in 2014 and 2019, respectively.

From November 2017 to November 2018, he was a visiting Ph.D. student with the University of Auckland, Auckland, New Zealand. From February 2022 to August 2022, he was a Visiting Scholar with the Yeungnam University, Kyongsan, Republic of Korea. He is currently an Associate Professor with the College of Mechanical and Electronic Engineering, Nanjing Forestry University, Nanjing. His current research interests include networked control systems, event-triggered control, and their applications.

Zhou Gu (Senior Member, IEEE) received the B.S. degree in automation from North China Electric Power University, Beijing, China, in 1997, and the M.S. and Ph.D. degrees in control science and engineering from the Nanjing University of Aeronautics and Astronautics, Nanjing, China, in 2007 and 2010, respectively.

From September 1999 to January 2013, he was with the School of Power engineering, Nanjing Normal University as an Associate Professor. He was a Visiting Scholar with Central Queensland University, Rockhampton, QLD, Australia, and The University of Manchester, Manchester, U.K. He is currently a Professor with the School of Electrical Engineering, Anhui Polytechnic University, Wuhu, China. He is also a Professor with Nanjing Forestry University, Nanjing. His current research interests include networked control systems, time-delay systems, reliable control, and their applications.

Ju H. Park (Senior Member, IEEE) received the Ph.D. degree in electronics and electrical engineering from the Pohang University of Science and Technology (POSTECH), Pohang, Republic of Korea, in 1997.

He was a Research Associate with the Engineering Research Center-Automation Research Center, POSTECH from May 1997 to February 2000. He joined Yeungnam University, Gyeongsan, Republic of Korea, in March 2000, where he is currently the Chuma Chair Professor. He is a coauthor of the monographs *Recent Advances in Control and Filtering of Dynamic Systems With Constrained Signals* (Springer Nature, New York, NY, USA, 2018) and *Dynamic Systems With Time Delays: Stability and Control* (Springer Nature, New York, 2019), and is an Editor of an edited volume *Recent Advances in Control Problems of Dynamical Systems and Networks* (Springer Nature, New York, 2020). His research interests include robust control and filtering, neural/complex networks, fuzzy systems, multiagent systems, and chaotic systems. He has published a number of articles in these areas. Since 2015, he has been a recipient of the Highly Cited Researchers Award by Clarivate Analytics (formerly, Thomson Reuters) and listed in three fields, Engineering, Computer Sciences, and Mathematics, from 2019 to 2022. He is also a Subject Editor/Advisory Editor/Associate Editor/Editorial Board Member of several international journals, including *IET Control Theory and Applications*, *Applied Mathematics and Computation*, *The Journal of The Franklin Institute*, *Nonlinear Dynamics*, *Engineering Reports*, *Cogent Engineering*, IEEE TRANSACTIONS ON FUZZY SYSTEMS, IEEE TRANSACTIONS ON NEURAL NETWORKS AND LEARNING SYSTEMS, and IEEE TRANSACTIONS ON CYBERNETICS. He is a Fellow of the Korean Academy of Science and Technology.

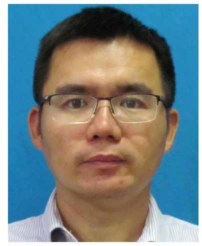

Xiangpeng Xie (Senior Member, IEEE) received the B.S. and Ph.D. degrees in engineering from Northeastern University, Shenyang, China, in 2004 and 2010, respectively.

From 2010 to 2014, he was a Senior Engineer with Metallurgical Corporation of China Ltd. He is currently a Professor with the School of Internet of Things, Nanjing University of Posts and Telecommunications, Nanjing, China. His research interests include fuzzy modeling and control synthesis, state estimation, optimization in process industries, and intelligent optimization algorithms. He serves as an Associate Editor for IEEE TRANSACTIONS ON INDUSTRIAL INFORMATICS, IEEE TRANSACTIONS ON FUZZY SYSTEMS, and IEEE TRANSACTIONS ON CYBERNETICS.

Wei Sun (Senior Member, IEEE) received the B.E. degree in automation, the M.S. degree in detection technology and automatic equipment, and the Ph.D. degree in electrical engineering from the Hefei University of Technology, China, in 2004, 2007, and 2012, respectively.

He is currently a Professor with the Hefei University of Technology. His research interests include wireless networks, networked control systems, and microgrids.